

Optical and structural properties of catalyst-free synthesized leaves like CdS films

S. H. MOHAMED^{a,b}, I. B. I. TOMSAH^a, M. EL-HAGARY^{a,c}

^aPhysics Department, College of Science, Qassim University, P. O. 6644, 51452, Buryadh, Kingdom of Saudi Arabia

^bPhysics Department, Faculty of Science, Sohag University, 82524 Sohag, Egypt

^cPhysics Department, Faculty of Science, Helwan University, 11792 Helwan, Cairo, Egypt

Leaves like CdS films were grown on catalyst-free Si(100) and quartz substrates by vapor transport of CdS powder at 850°C. Randomly aligned nanoleaves with different shapes were observed. X-ray diffraction analysis revealed that the leaves like CdS is a single phase nature with hexagonal crystal structure. The optical functions of CdS films have been determined by ellipsometry investigations from 400 - 1100 nm. A two layer model employing the Cauchy dispersion model for the main layer and Bruggeman effective medium approximation (BEMA) for the surface layer was found to be sufficient and reasonable. The obtained optical constants were compared with those obtained by other preparation methods. The transmittance has high values while the reflectance has low values in the wavelength range 450 – 2500 nm. A direct optical band gap value of 2.41 eV and Urbach energy of 2671 meV were obtained.

(Received April 24, 2013; accepted July 11, 2013)

Keywords: Vapor transport, CdS nanoleaves, Optical constants

1. Introduction

Semiconductor nanocrystals (dots, rods, wires, etc.) exhibit a wide range of electrical and optical properties that differ from those of the corresponding bulk materials. These properties depend on both nanocrystal (NC) size and shape [1]. In the last decade, there were increased research activities on dimensionality control of NC properties, since the electrons interact differently in nanostructures having different dimensionality. One- or two dimensional systems are critical to the function and integration of nanoscale devices since these are the lowest dimensional structures that can be used for efficient transport of electrons and optical excitations [2]. Compared with zero-dimensional (0D) quantum dots, 1D nanostructures such as nanorods, nanowires and nanoleaves have reduced symmetry and an additional degree of freedom, i.e., the length or aspect ratio. They are capable of exhibiting physical phenomena, such as linearly polarized light emission, that are not observed in spherical nanocrystals. Semiconductor nanorods and nanowires have been attracting great interest for applications in nanoelectronics, photonics, data processing, and biological and medical sensing.

To date, significant progress has been made in the fabrication of 1D nanostructures for a variety of materials, mainly semiconductors but also including metals and metal oxides. Several approaches are commonly used for the generation of 1D nanostructures, including surfactant controlled growth, growth with catalysts (solution-liquid-solid, SLS and vapor liquid solid, VLS), growth by oriented attachment, templated growth and growth in the presence of an external field [3-7]. Of these methods, the

first two are the most commonly used techniques for the synthesis of 1D nanostructures.

CdS is a II VI semiconductor with a Bohr radius of 2.4 nm [8] and a direct band gap of 2.4 eV [9]. It can be used in photocatalytic hydrogen production and electricity generation [10], in thin film transistors [11], in light-emitting diodes, and in other nonlinear optical devices [12,13]. CdS nanorods or nanowires can be prepared by several approaches, including laser assisted catalytic growth [14], thermal evaporation of CdS nanopowders [15], templated growth [16,17] and solvothermal routes [10, 18]. However, previous studies were mostly focused on nanoparticles, and the common synthesis method is a soft chemistry approach. In this paper, CdS leaves like is reported by a simple one-step thermal evaporation method without using a catalyst. The structural and optical properties of CdS nanoleaves were studied.

2. Experiment

CdS powder (99.995% purity, Aldrich chemicals) was placed in an alumina boat that was inserted into the center of a quartz tube (inner diameter of 25 mm and length of 60 cm) which being put into horizontal tube furnace. The end of the quartz tube was left open. The synthesis was carried out on ultrasonically cleaned Si (100) and quartz substrates (cut into 1 × 1 cm²). The cleaned substrates were put approximately 6 cm away and a long 14 cm distance from the alumina boat. The growth was carried out at 850 °C using 300 sccm (standard cubic centimeter per minute) Ar. The growth time was 1 h, after that the furnace was cooled down to room temperature.

The surface morphology of the synthesized nanostructures was characterized by scanning electron microscope (SEM) type JOEL model JSM 5300 (Japan). The crystal structure was investigated by X-ray diffraction (XRD) using a Philips-PW1710 X-ray diffractometer which utilizing CuK_α radiation ($\lambda = 1.541838 \text{ \AA}$). The chemical composition of the synthesized nanostructures was analyzed using energy dispersive analysis of X-ray (EDAX) unit attached with the SEM.

The spectroscopic ellipsometry (SE) data for the prepared nanostructured films at different positions were acquired using a PHE-102 variable angle spectroscopic ellipsometer (Angstrom Advanced Inc.) in the wavelength range 400 - 1100 nm (energy range 3.10 - 1.13 eV). The data were acquired at angle of incidences of 60° , 65° and 70° . The instrument measures the complex ratio of the Fresnel reflection coefficients for p-and s-polarized light and reports the ratio in terms of the ellipsometric parameters ψ and Δ defined by the equation

$$F = \tan(\Psi) \exp(i\Delta) = \frac{\tilde{r}_p}{\tilde{r}_s} \quad (1)$$

where \tilde{r}_p and \tilde{r}_s are the amplitude reflection coefficient for light polarized in the p-and s- plane of incidence, respectively. The data obtained from the ellipsometer were accurately modeled using the PHE-102 software package. Ellipsometric data ψ and Δ for variable wavelengths were fitted in the optical model. The spectral transmittance (T%) and reflectance (R%) of CdS films were obtained through JASCO V-670 double beam spectrophotometer. The measurements were performed in the wavelength range from 190 to 2500 nm. The transmittance spectrum was recorded at normal incidence, while the reflectance spectrum was recorded at 6° of the normal to the sample surface.

3. Results and discussions

3.1 Surface morphology, compositional and structural examinations

Observations with scanning electron microscopy (Fig. 1a-b) clearly show a general view of randomly aligned nanoleaves with different shapes. The widths of the leaves are ranged from 75 nm to 6.5 μm and lengths extending to several tens of micrometers. The corresponding EDAX data shown in Fig. 1c confirms the existence of Cd and S. In addition to these, signals from Si and C elements were also observed, which presumably could have appeared from the silicon substrate and the hydrocarbons contamination, respectively. The sources of hydrocarbons are the carbon dioxide and water molecules. The contamination by hydrocarbons could have happened either during preparation by the adsorbed carbon dioxide and water on the walls of the preparation tube or after the samples were subjected to atmospheric air. Within a precision of 2 at.%, the Cd and S atomic percentages are

found to be 58.94% and 41.16%, respectively. Thus, the molecular ratio of S/Cd of the nanoleaves calculated from the EDAX quantitative analysis data is less than that of a stoichiometric CdS crystal. The loss of S may be ascribed to the reaction of some of the evaporated S atoms with the residual oxygen in the reactor tube according to the following formula:



Then, the SO_2 may get out of the reactor tube.

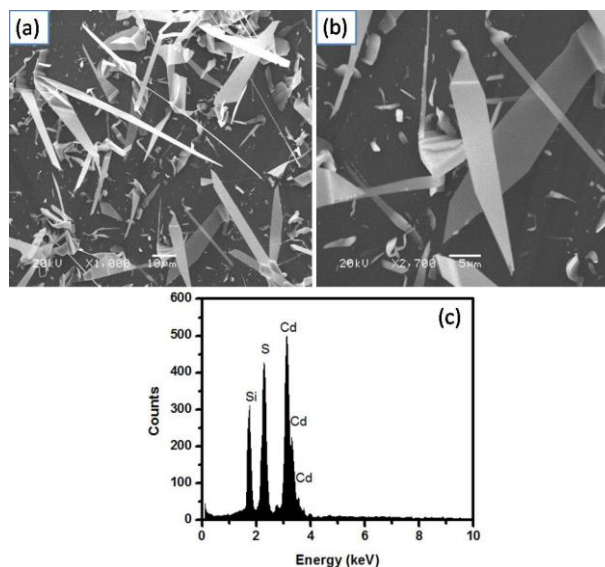


Fig. 1. SEM images (a,b) and EDAX spectra (c) of the deposited nanostructured CdS samples on Si(100) substrates.

The X-ray diffraction pattern of CdS nanostructured is shown in Fig. 2. From the pattern it is clear that the sample is polycrystalline in nature. All peaks from the diffraction pattern are characteristic of hexagonal CdS phase (JCPDS card no. 77-2306). Although EDAX analysis revealed an excess of Cd, no diffraction peaks of Cd is detected revealing that the product is of the pure hexagonal CdS phase. The excess Cd atoms may segregate to the noncrystalline regions in grain boundaries.

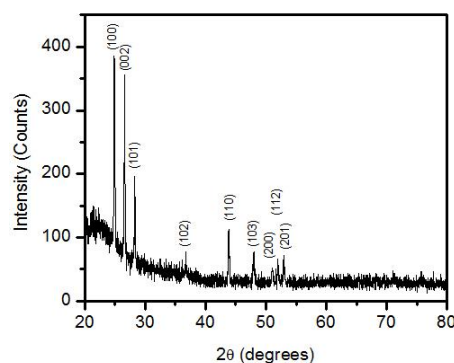


Fig. 2. XRD patterns of the deposited leaves like CdS film on quartz substrate.

The texture coefficient $P(h_i k_i l_i)$, a preferential orientation indicator of the $(h_i k_i l_i)$ plane, is given by the following equation [19]:

$$P(h_i k_i l_i) = \left(\frac{I(h_i k_i l_i)}{I_r(h_i k_i l_i)} \right) \left(\frac{1}{m} \sum_{i=1}^m \frac{I(h_i k_i l_i)}{I_r(h_i k_i l_i)} \right)^{-1} \quad (2)$$

where $I(h_i k_i l_i)$ is the diffraction intensity of the $(h_i k_i l_i)$ plane of the sample under investigation, $I_r(h_i k_i l_i)$ is the intensity of the $(h_i k_i l_i)$ plane of a random powder sample and m is the number of diffraction peaks. Equation 2 shows that $P(h_i k_i l_i)$ of each crystallographic plane is unity for a randomly distributed powder sample, and is larger than unity if $(h_i k_i l_i)$ plane is preferentially oriented. The Harris analysis results are summarized in Table 1. Apparently, the texture coefficient value of the index (002) plane for hexagonal CdS is the highest indicating that is more preferentially oriented.

Table 1. X-ray diffraction intensities and preferred orientation factors of CdS nanoleaves.

(hkl)	I	I_r^{**}	P_{hkl}
(100)	100	63	1.70
(002)	92	45	2.18
(101)	51	100	0.54
(102)	20	25	0.85
(110)	29	43	0.72
(103)	20	41	0.52
(200)	9	6	1.60
(112)	17	31	0.59
(201)	19	13	1.56

** From JCPDS, International Centre for Diffraction Data, 1996.

3.2 Optical properties examinations

SE spectra of CdS film, on Si(100) substrate, in the wavelength range of 400–1100 nm is shown in Fig. 3. The experimental data were analyzed using a procedure which considers that the film is made of two layers; an inner compact layer and an outer porous layer [20]. The Cauchy-Urbach dispersion relation was used to describe the complex refractive index of the compact layer and the Bruggeman effective medium approximation was used to describe the complex refractive index of the porous layer. A good fit was found between the model and experimental data. Thickness of CdS main layer is found to be 102.2 nm and the surface roughness layer is 6.3 nm.

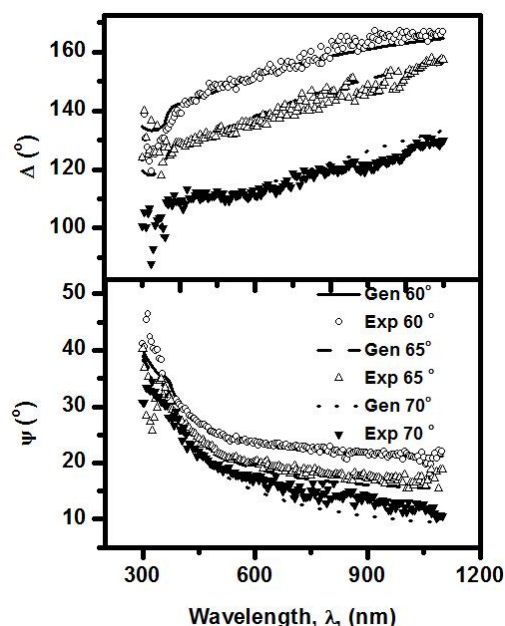


Fig. 3. An example for the best fit of the experimental Ψ and Δ of the leaves like CdS film on Si(100) substrate.

Refractive index (n) and extinction coefficient values of CdS film are given in Fig. 4a-b. The refractive index (Fig. 4a) increases with increasing wavelength up to 485 nm, then it continuously decreases with increasing wavelength. The refractive index value at 600 nm is 1.704 which is lower than the value 2.238 obtained for the chemical bath deposition CdS films [21], however the overall obtained n values are greater than the values obtained for CdS films prepared by ultrasonic spray pyrolysis technique [22]. The extinction coefficient (k) (Fig. 4b) decreases with increasing wavelength and reaches close to zero at higher wavelengths.

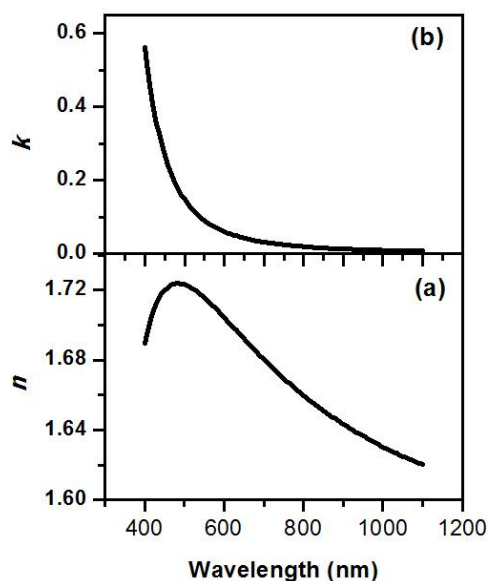


Fig. 4. Variations of the refractive index (a) and extinction coefficient (b) as function of wavelength for the deposited leaves like CdS film.

Fig. 5 shows the variations of transmittance (T) and reflectance (R) as a function of wavelength in the range 200–2500 nm. The transmittance has high values while the reflectance has low values in the wavelength range 450–2500 nm. A sharp absorption edge is observed below 400 nm. Using the measured spectral transmittance and reflectance, and the film thickness (d) the absorption coefficient (α) was calculated according to

$$\alpha = \frac{1}{d} \ln \left(\frac{1-R}{T} \right) \quad (3)$$

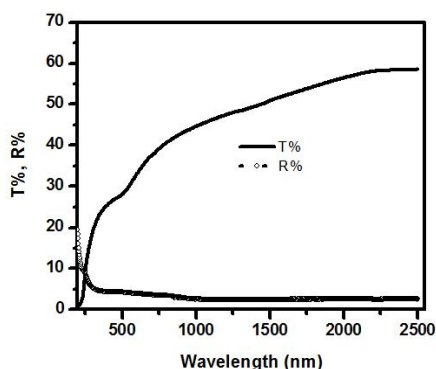


Fig. 5. Variations of transmittance (T) and reflectance (R) as a function of wavelength for the deposited leaves like CdS film on quartz substrate.

The thickness derived for the SE was used. The optical band gap (E_g) was determined using the following formula

$$(\alpha h\nu)^2 = \beta(h\nu - E_g) \quad (4)$$

where β is a constant and h is Planck's constant. The E_g values are extracted from the $(\alpha h\nu)^2$ versus $h\nu$ plot as shown in Fig. 6a. The obtained E_g value is 2.41 eV. This value is close to the values 2.39 eV and 2.45 eV obtained for CdS nanocrystalline thin films prepared by sol-gel dip-coating method [23] and spray pyrolysis technique [24], respectively.

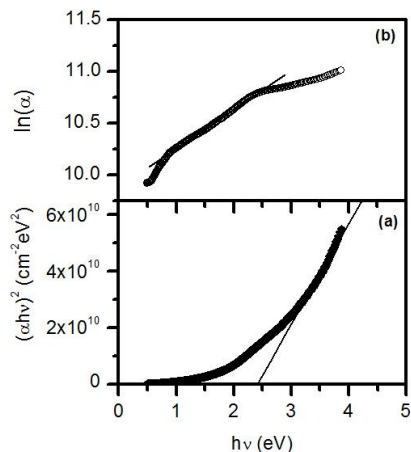


Fig. 6. Plots of $(\alpha h\nu)^2$ versus $h\nu$ (a) and $\ln(\alpha)$ versus $h\nu$ (b) for the deposited leaves like CdS film.

The absorption coefficient (α) near the fundamental absorption edge usually shows simple exponential energy dependence referred to as the Urbach tail

$$\alpha = K \exp(E/E_u) \quad (5)$$

where K is constant and E_u is Urbach energy which is interpreted as the width of the tails of localized states in the band gap [25]. The absorption in this region is due to transitions between extended states in one band and localized states in the exponential tail of the other band as well as the effects of all defects [26]. Plotting $\ln \alpha$ as a function of energy, as shown in Fig. 6b, the E_u can be calculated. The obtained E_u value is 2671 meV. The obtained E_u value for the CdS nanoleaves is higher than the reported value, 158 meV, for the sol-gel prepared CdS nanoparticles [23].

4. Conclusion

Leaves like CdS was synthesized by the evaporation condensation method on catalyst free Si(100) and quartz substrates. The XRD and EDAX analysis revealed the presence of single crystalline phase of hexagonal CdS structure with lower S content. The thickness and optical constants were accurately determined from the SE which may prove useful in the design of nano-optoelectronic devices. The optical band gap and the Urbach energy were calculated.

Acknowledgments

This work is supported by the Deanship of Scientific Research at Qassim University under contract number 1869.

References

- [1] A. P. Alivisatos, *Science* **271**, 933 (1996).
- [2] J. T. Hu, T. W. Odom, C. M. Lieber, *Acc. Chem. Res.* **32**, 435 (1999).
- [3] P. D. Cozzoli, T. Pellegrino, L. Manna, *Chem. Soc. Rev.* **35**, 1195 (2006).
- [4] C. J. Murphy, N. R. Jana, *Adv. Mater.* **14**, 80 (2002).
- [5] C. Yang, M. Li, W.-H. Zhang, C. Li, *Sol. Energ. Mat. Sol. Cells* **115**, 100 (2013).
- [6] S. H. Mohamed, *J. Alloys Compd.* **510**, 119 (2012).
- [7] S. H. Mohamed, *Phil. Mag.* **91**, 3598 (2011).
- [8] J. Z. Zhang, *J. Phys. Chem. B* **104**, 7239 (2000).
- [9] G. Z. Shen, J. H. Cho, J. K. Yoo, G. C. Yi, C. J. Lee, *J. Phys. Chem. B* **109**, 9294 (2005).
- [10] J. S. Jang, U. A. Joshi, J. S. Lee, *J. Phys. Chem. C* **111**, 13280 (2007).
- [11] Ji-Hye Kwon, Joo-Seob Ahn, Heesun Yang, *Current Appl. Phys.* **13**, 84 (2013).
- [12] L. Weinhardt, T. Gleim, O. Fuchs, C. Heske, E. Umbach, M. Bar, H. J. Muffler, C. H. Fischer, M. C. Lux-Steiner, Y. Zubavichus, T. P. Niesen, F. Karg,

- Appl. Phys. Lett. **82**, 571 (2003).
- [13] S. Mandal, D. Rautaray, A. Sanyal, M. Sastry, J. Phys. Chem. B **108**, 7126 (2004).
- [14] X. F. Duan, C. M. Lieber, Adv. Mater. **12**, 298 (2000).
- [15] C. H. Ye, G. W. Meng, Y. H. Wang, Z. Jiang, L. D. Zhang, J. Phys. Chem. B **106**, 10338 (2002).
- [16] J. W. Grebinski, K. L. Richter, J. Zhang, T. H. Kosel, M. Kuno, J. Phys. Chem. B **108**, 9745 (2004).
- [17] M. F. Zhang, M. Drechsler, A. H. E. Muller, Chem. Mater. **16**, 537 (2004).
- [18] F. Liu, X. Shao, J. Wang, S. Yang, H. Li, X. Meng, X. Liu, M. Wang J. Alloys Compd. **551**, 327 (2013).
- [19] C. S. Barrett, T. B. Massalski, "Structures of metals", (Pergamon, Oxford, 1980) p. 204.
- [20] S. H. Mohamed, M. El-Hagary, S. Althoyaib, J. Alloys Compd. **537**, 291 (2012).
- [21] H. Metin, R. Esen, J. Cryst. Growth **258**, 141 (2003).
- [22] S. Kose, F. Atay, V. Bilgin, I. Akyuz, E. Ketenci, Appl. Surf. Sci. **256**, 4299 (2010).
- [23] A. A. Ziabari, F. E. Ghodsi, J. Lumin. **141**, 121 (2013).
- [24] A. Rmili, F. Ouachtari, A. Bouaoud, A. Louardi, T. Chtouki, B. Elidrissi, H. Erguig, J. Alloys. Compd. **557**, 53 (2013).
- [25] J. C. Tauc, Optical Properties of Solids, North-Holland, Amsterdam, 1972; J. C. Tauc, Amorphous and Liquid Semiconductors, Plenum Press, New York, 1974.
- [26] V. Srikant, D. R. Clarke, J. Appl. Phys. **81**, 6357 (1997).

*Corresponding author: abo_95@yahoo.com